N90-24000

PLATINIZED TIN OXIDE CATALYSTS FOR CO_2 LASERS: EFFECTS OF PRETREATMENT

Steven D. Gardner and Gar B. Hoflund
Department of Chemical Engineering
University of Florida
Gainesville, Florida

David R. Schryer and Billy T. Upchurch
NASA Langley Research Center
Hampton, Virginia

ABSTRACT

$Pt/SnO_2/SiO_2$ surfaces used for low-temperature CO oxidation in CO_2 lasers have been characterized before and after reduction in CO at 125 and 250°C using ion scattering spectroscopy (ISS) and X-ray photoelectron spectroscopy (XPS). XPS indicates that the Pt is present initially as PtO_2. Reduction at 125°C converts the PtO_2 to $Pt(OH)_2$ while reduction at 250°C converts the PtO_2 to metallic Pt. ISS results suggest tht during the 250°C reduction the Pt and Sn in the outermost atomic layer of the catalyst are covered by impurities originating from the silica substrate. The XPS results are consistent with partial SnO_2 reduction to SnO. The surface dehydration, change of Pt chemical state, and migration of substrate impurities over surface Pt and Sn appear to explain why a CO pretreatment at 250°C produces inferior CO oxidation activity compared to a 125°C CO pretreatment.

INTRODUCTION

The catalyzed oxidation of CO has important applications for closed-cycle, pulsed CO_2 lasers (1,2). In order to maintain power during the sealed operation of a CO_2 laser, it is necessary to recombine CO and O_2 which are produced during the laser discharge because the O_2 quenches the lasing action. This reaction may be brought about through the integration of an appropriate CO-oxidation catalyst within the CO_2 laser unit. Such an approach preserves the discharge quality of the laser while the advantages of sealed operation are maintained.

Research has indicated that platinized tin oxide is an efficient CO-oxidation catalyst at conditions which correspond to steady-state CO_2 laser operation (1,3). Although the performance of Pt/SnO_2 has been maximized, efforts to understand the reaction mechanism continue. It has been demonstrated that the activity of Pt/SnO_2 towards CO oxidation is a strong function of pretreatment procedures (4). For example, a reductive pretreatment using CO or H_2 produces superior activity relative to an inert or oxidative pretreatment or no pretreatment at all. The pretreatment temperature influences the catalytic performance as well. Compared with high-temperature reductions, low-temperature reductions near 125°C produce surfaces which are more active. For CO reductions above about 175°C, a sharp, temporary decrease in activity is observed initially. This induction period is believed to be the result of surface dehydration caused by combination and desorption of surface hydroxyl groups (4). No significant induction period results when Pt/SnO_2 is

humidified either after CO pretreatment or during the reaction itself. The data obtained thus far also suggest that optimum pretreatment times exist which is consistent with the hypothesis involving surface dehydration. While the exact function of surface hydroxyl groups in the overall reaction remains unknown, it is thought that OH^- groups might serve as oxidants for CO chemisorbed on Pt (4,5). There is also evidence which suggests that OH^- may stabilize a carbonate complex which ultimately decomposes to yield CO_2 (6).

Acknowledging the importance of surface hydroxyl groups, there has been considerable effort directed towards the development of a platinized tin oxide catalyst which is supported on a silica substrate (7). It is hypothesized that the hygroscopic silica may benefit Pt/SnO_2 by preventing extensive surface dehydration and consequent activity loss. Experiments have been conducted wherein the catalyst performance has been optimized with respect to several variables including pretreatment procedures. Superior performance is realized from a reductive pretreatment in 5% CO/He at 125°C for 1 hour. As pretreatment temperatures approach 250°C there is a significant decrease in the observed activity. Although not as active as Au/MnO_x (8), the optimized $Pt/SnO_2/SiO_2$ catalyst represents a significant improvement over commercially available Pt/SnO_2 with respect to low-temperature CO oxidation activity and performance decay (5).

In order to explain these experimental observations, it is necessary to characterize the catalyst surface species which are present before and after a given pretreatment procedure. The present study utilized ion scattering spectroscopy (ISS) and X-ray photoelectron spectroscopy (XPS) to examine the concentrations and chemical states of surface species associated with a $Pt/SnO_2/SiO_2$ catalyst as a function of CO pretreatment temperature.

EXPERIMENTAL

The catalyst prepared for this study consisted of a thin layer of platinum and tin oxide dispersed on a silica gel substrate (7). The silica gel was impregnated with tin oxide via evaporation of a stirred solution of tin metal powder and silica gel in concentrated nitric acid at 150°C. Subsequently, platinum was precipitated from an aqueous solution of platinum tetraamine dihydroxide and formic acid with heating followed by drying at 150°C. The final product was heated in air at 150°C for 4 hours.

Two as-prepared $Pt/SnO_2/SiO_2$ samples were inserted into an ultrahigh vacuum (UHV) system (base pressure of 10^{-11} Torr). After initial surface characterization, the samples were each transferred into a preparation chamber connected to the UHV system and reduced in 10 Torr of CO for two hours at 125 and 250°C. Heating was accomplished via conduction from a platform heating element which was resistively heated (9) in order to avoid dissociating the reducing gas. Sample temperatures were measured using a thermocouple attached to the stainless steel sample support block. After reduction, each sample was returned to the UHV chamber without air exposure for further characterization.

Energy analysis for the ISS and XPS experiments was accomplished using a Perkin-Elmer PHI Model 25-270 double-pass cylindrical mirror analyzer (CMA). The CMA contained an internal, movable aperture which varied the polar acceptance angle for incoming particles. ISS spectra were collected in the nonretarding mode using a 147° scattering angle and pulse counting detection

(10). A 100 nA, 1 keV $^4He^+$ primary beam was defocused over a 1 cm^2 area to minimize sputter damage. Survey and high-resolution XPS spectra were recorded with Mg Ka excitation in the retarding mode using 50 and 25 eV pass energies respectively.

RESULTS AND DISCUSSION

XPS survey spectra taken before and after CO reduction from two $Pt/SnO_2/SiO_2$ catalyst samples appear in figures 1 and 2 respectively. The two catalyst samples examined (designated as samples A and B) were similar in that both were randomly dispensed from the same catalyst batch. For the air-exposed surfaces, the spectra in figures 1a and 2a exhibit predominant peaks due to Sn and O while peaks due to Pt are present but less discernible. Differences between figures 1a and 2a with regard to the O/Sn ratio suggest that the as-prepared catalyst samples lack uniformity in average surface composition. Nevertheless, important information may still be obtained with respect to data taken from each catalyst sample before and after reduction. A thick tin oxide surface layer (> 50 angstroms) is indicated by the lack of Si XPS signals arising from the silica substrate. Only trace amounts of carbon and surface contaminants are detected. Reduction in CO results in changes in the Sn and O signals as shown in figures 1b and 2b. The spectra indicate that the surface region of sample A (reduced at 125°C) becomes oxygen-enriched while surface oxygen depletion occurs in sample B (reduced at 250°C). A possible mechanism responsible for this result is discussed below.

ISS spectra taken from sample B before and after reduction appear in figures 3a and 3b respectively. Figure 3a reveals distinct Pt and O features while the Sn peak appears as a shoulder on the Pt peak. After catalyst reduction, figure 3b indicates that the surface composition has changed considerably. The Pt and Sn peaks have decreased in intensity and a new group of peaks has emerged centered near 0.55 E/E_o. Although features due to Si would appear in this region, it is most probable that these peaks are due to impurities commonly associated with silica such as sodium. Considering the stability of silica, it seems unlikely that silica species would migrate to any appreciable extent under these pretreatment conditions. Since ISS is essentially sensitive to the outermost layer of surface atoms, the data in figure 3 suggest that the 250°C reduction results in physical coverage (encapsulation) of the majority of surface Pt and Sn. This encapsulation hypothesis is confirmed by an ISS experiment performed after the reduced surface was lightly sputtered. As shown in figure 4, the sputtering process uncovered significant amounts of underlying Pt and Sn. Although surface charging features appear in these ISS spectra, the peaks which correspond to Pt and Sn remain prominent and meaningful.

The data presented thus far suggest that a 250°C CO reduction promotes movement between Pt and Sn at the surface and underlying impurities contained within the silica substrate. The resulting migration of substrate species over surface Pt and Sn is consistent with the more bulk-sensitive XPS results in figures 2a and 2b. As discussed below, oxygen migration from the subsurface region may also be important as the reduction of Pt proceeds. However, changes due to surface desorption mechanisms cannot be ruled out and most likely are important. A consistent observation is that oxygen surface desorption as well as bulk diffusion processes are more prevalent at 250°C than at 125°C which would explain the overall trend that is observed in the XPS survey

spectra. At 125°C surface desorption mechanisms do not appear to be significant, and as a result XPS indicates that migrating oxygen species concentrate near the surface resulting in the increased O-to-Sn peak height ratio. Whether substrate coverage of surface Pt and Sn is extensive at 125°C is uncertain due to the lack of ISS data for sample A.

High resolution XPS spectra of the O 1s features are shown in figures 5 and 6. The fact that two distinct O 1s peaks appear is unusual and suggests that differential charging is occurring. Differential charging is indicative of an insulating surface which tends to acquire a steady-state charge during analysis. A net surface charge may result from an unbalance between photoelectron loss and electron gain from the immediate environment. When such complications arise peak binding energies shift proportionately to the extent of surface charging thus requiring correction. As indicted, these two peaks are obtained from both samples both before and after reduction. However, during catalyst reduction, the peak separations decrease from about 9 eV to 7.3 eV with the smaller peak remaining essentially stationary in binding energy. Therefore differential charging appears less severe on the reduced samples indicating that these surfaces are more metallic in nature (although they remain predominantly insulating). As shown in figure 7, the Pt 4f XPS spectra exhibit broad features suggesting that multiple Pt oxidation states are present even after reduction. Due to charging effects, however, the corresponding binding energies require correction. It is interesting to note the results when the Pt 4f spectra taken before and after reduction are corrected, respectively, by the 9 and 7.3 eV oxygen peak separations noted above. Adjusted for surface charging accordingly, figure 7a indicates that a mixture of PtO_2, PtO and perhaps $Pt(OH)_2$ is present on the air-exposed surfaces. After oxidation, peak positions shift toward lower binding energies as surface Pt is partially reduced. After reduction at 125°C, figure 7b indicates a major peak corresponding to $Pt(OH)_2$, while figure 7c reveals that metallic Pt is dominant after the 250°C reduction. A comparison of figures 7b and 7c suggests that increasing the CO reduction temperature from 125°C to 250°C seems to increase the extent to which Pt is reduced, although in either case multiple Pt states remain.

The Sn 3d XPS spectra taken before and after reduction from both samples appear in figures 8 and 9. After reduction, the spectra in both figures indicate a peak shift which is essentially equal to the 1.7 eV oxygen peak shift noted above. Although metallic and oxidic Sn exhibit approximately this ame peak shift, the overall conservation of peak shape and character which is depicted suggests that the peak shift results from the aforementioned surface charging effects. Therefore, it appears that most of the Sn remains essentially oxidic in nature during CO reduction at both temperatures. However, the Sn 3d peaks become slightly wider along the low-binding energy side as the reduction temperature increases indicating that a very small amount of Sn may have been reduced. Several possibilities exist regarding the form of the reduced Sn. There is evidence that metallic Sn and possibly alloyed Sn form when platinized tin oxide surfaces are annealed in vacuum near 450°C (11). Similar conclusions have been reached when a commercial Pt/SnO_2 catalyst is reduced in CO at temperatures up to 175°C (5). In both cases, however, the metallic or alloyed Sn appeared as a baseline shoulder on the low-binding energy side of the tin oxide Sn 3d XPS peaks. After CO reduction in the present study, the overall character of the tin oxide Sn 3d peaks is somewhat different with the entire low-binding energy side exhibiting a broadened

appearance. Paparazzo and coworkers (12) have noted similar results using XPS to study air-exposed and annealed SnO_2 and SnO surfaces. Their XPS experiments were able to discern SnO_2 from SnO and metallic Sn. The annealed surfaces exhibited metallic features which emerged as distinct peaks or shoulders near the baseline of the respective tin oxide Sn $3d_{5/2}$ peaks. Quite unlike the metallic features, the spectral contrasts observed between SnO_2 and SnO appeared as nominal shifts over the entire Sn $3d_{5/2}$ peaks. The latter observation is more consistent with the results observed in this study. The data in figures 7 and 8 therefore suggest that during the pretreatments a small fraction of SnO_2 may have been reduced to some lower oxide of Sn such as SnO.

The XPS data are consistent with the suggestion that surface hydroxyl groups facilitate CO oxidation on platinized tin oxide catalysts (4). After CO reduction, a greater oxygen surface concentration is indicated for sample A relative to sample B. Hydrogen should also be present at these temperatures (13). The superior performance which results from a 125°C CO pretreatment may therefore be attributed to hydroxyl groups which are not desorbed at these pretreatment conditions. It is also unlikely that encapsulation occurs at the lower temperature. Indeed, assuming that the charge corrections to the Pt 4f XPS features are valid, the spectra indicate that a greater concentration of surface $Pt(OH)_2$ is present after the 125°C CO reduction.

A related study by Drawdy et al. (5) is consistent with much of the data presented above. In that study a 2 wt% Pt/SnO_2 catalyst (Engelhard Corporation) was characterized using ISS, XPS and Auger electron spectroscopy (AES) after CO reductive pretreatments at 75, 100, 125 and 175°C. Coincident with increasing reduction temperature was an increase in the concentration of surface $Pt(OH)_2$ species. XPS indicated that $Pt(OH)_2$ is the predominant Pt specie after reduction at 175°C. It is interesting that pretreatments near 175°C promote superior activity enhancement for the Engelhard Pt/SnO_2 catalyst. In fact nearly identical activity enhancement is observed for pretreatments between 125 and 225°C. Therefore, with respect to both catalysts, these two studies suggest that the pretreatments which favor $Pt(OH)_2$ formation on the catalyst surface are the most beneficial. Apparently, the Pt/SnO_2 catalyst continues to benefit from pretreatments at higher temperatures since it does not undergo interactions with a silica substrate.

It is important to emphasize that the benefits of these reductive pretreatments are realized only after several hours of reaction. During this period the surface may undergo significant changes with respect to the types of surface species present and their chemical states. Further research is in progress which will characterize the surfaces of these pretreated catalysts as a function of reaction time. Additional pretreatment temperatures are also being investigated to further examine the surface alterations described above.

SUMMARY

The effects of two CO pretreatment temperatures on a $Pt/SnO_2/SiO_2$ surface have been examined using ISS and XPS. A CO reduction at 250°C promotes migration of silica substrate impurities over surface Pt and Sn while depleting the surface region of oxygen. At 125°C, CO reduction results in surface oxygen enrichment. Subsequent to both CO reductions, most of the Sn appears to remain oxidic while surface Pt is only partially reduced. Increasing the CO reduction temperature increases the extent to which the Pt is reduced. After

a 125°C reduction, $Pt(OH)_2$ appears dominant while after a 250°C reduction most of the Pt is in metallic form. The data are consistent with a dual mechanism which suggests that surface dehydration and substrate migration over surface Pt and Sn are responsible for the inferior CO oxidation activity produced by a 250°C CO pretreatment. The XPS results are consistent with partial SnO_2 reduction to SnO but more direct evidence would be desirable.

REFERENCES

1. "Closed-Cycle, Frequency-Stable CO_2 Laser Technology, Proceedings of a workshop held at Langley Research Center, Hampton, VA, June 10-12, 1986," C.E. Batten, I.M. Miller and G.M. Wood, Jr., eds., NASA Conference Publication 2456.

2. D.S. Stark, A. Crocker and G.J. Steward, "A sealed 100-Hz CO_2 laser using high CO_2 concentrations and ambient temperature catalysis," J. Phys. E: Sci. Instrum. 16, 158-161 (1983).

3. D.S. Stark and M.R. Harris, "Catalysed recombination of CO and O_2 in sealed CO_2 TEA laser gases at temperatures down to -27°C," J. Phys. E: Sci. Instrum. 16, 492-496 (1983).

4. D.R. Schryer, B.T. Upchurch, J.D. Van Norman, K.G. Brown and J. Schryer, "The effects of pretreatment conditions on a Pt/SnO_2 catalyst for the oxidation of CO in CO_2 lasers," J. Catal. 00, 00 (1990).

5. J.E. Drawdy, G.B. Hoflund, S.D. Gardner, E. Yngvadottir and D.R. Schryer, "Effect of Pretreatment on a Platinized Tin Oxide Catalyst used for Low-Temperature CO Oxidation," Surface and Interface Analysis 00, 00 (1990).

6. C.H.F. Peden and J.E. Houston, "Identification of a Carbonate Species during CO Oxidation on Deactivated Rh(111)," to be published.

7. B.T. Upchurch, D.R. Schryer, G.M. Wood and R.V. Hess, "Development of CO oxidation catalysts for the Laser Atmospheric Wind Sounder (LAWS)," in Proceedings of SPIE - International Society for Optical Engineering: Laser Applications in Meteorology and Earth and Atmospheric Remote Sensing, edited by M.M. Sokoloski, published by SPIE, Bellingham, Washington, 1062, 287 (1989).

8. S.D. Gardner, G.B. Hoflund, D.R. Schryer, J. Schryer, B.T. Upchurch, and D.R. Brown, "The Catalytic Behavior of Noble Metal/Reductible Oxide Materials for Low-Temperature CO Oxidation," submitted to Langmuir.

9. G.B. Hoflund, G.R. Corallo and M.R. Davidson, to be published.

10. R.E. Gilbert, D.F. Cox and G.B. Hoflund, "Computer-interfaced digital pulse counting circuit," Rev. Sci. Instrum. 53(8), 1281 (1982).

11. S.D. Gardner, G.B. Hoflund, M.R. Davidson and D.R. Schryer, "Evidence of Alloy Formation during Reduction of Platinized Tin Oxide Surfaces," J. Catal. 115, 132 (1989).

12. E. Paparazzo, G. Fierro, G.M. Ingo and N. Zacchetti, "XPS Studies on the Surface Thermal Modifications of Tin Oxides," Surface and Interface Analysis 12, 438 (1988).

13. G.B. Hoflund, A.L. Grogan, Jr., D.A. Asbury and D.R. Schryer, "A Characterization Study of a Hydroxylated Polycrystalline Tin Oxide Surface," Thin Solid Films 169, 69 (1989).

FIGURE CAPTIONS

Figure 1. XPS survey spectra taken from the platinized tin oxide surface of sample A (a) before and (b) after CO reduction at 125°C.

Figure 2. XPS survey spectra taken from the platinized tin oxide surface of sample B (a) before and (b) after CO reduction at 250°C.

Figure 3. ISS spectra taken from sample B (a) before and (b) after CO reduction at 250°C.

Figure 4. ISS spectrum taken from sample B after reduction and subsequent sputtering with 2 keV, 40 mA $^4He^+$ ions for 5 minutes using a beam current of 10 μA over a 1 cm^2 area.

Figure 5. O 1s XPS spectra taken from sample A (a) before and (b) after CO reduction at 125°C.

Figure 6. O 1s XPS spectra taken from sample B (a) before and (b) after CO reduction at 250°C.

Figure 7. Pt 4f XPS spectra taken from (a) the as-entered platinized tin oxide surface, (b) sample A after CO reduction at 125°C and (c) sample B after CO reduction at 250°C.

Figure 8. Sn 3d XPS spectra taken from sample A (a) before and (b) after CO reduction at 125°C.

Figure 9. Sn 3d XPS spectra taken from sample B (a) before and (b) after CO reduction at 250°C.

#A2, p-1

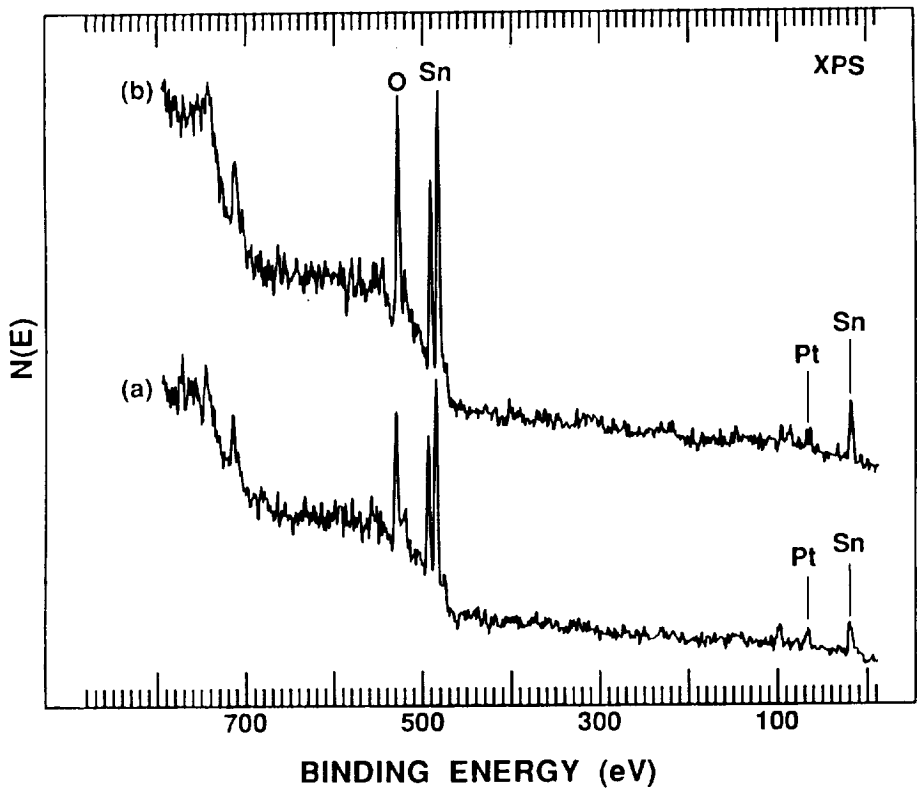

Figure 1. XPS survey spectra taken from the platinized tin oxide surface of sample A (a) before and (b) after CO reduction at 125 °C.

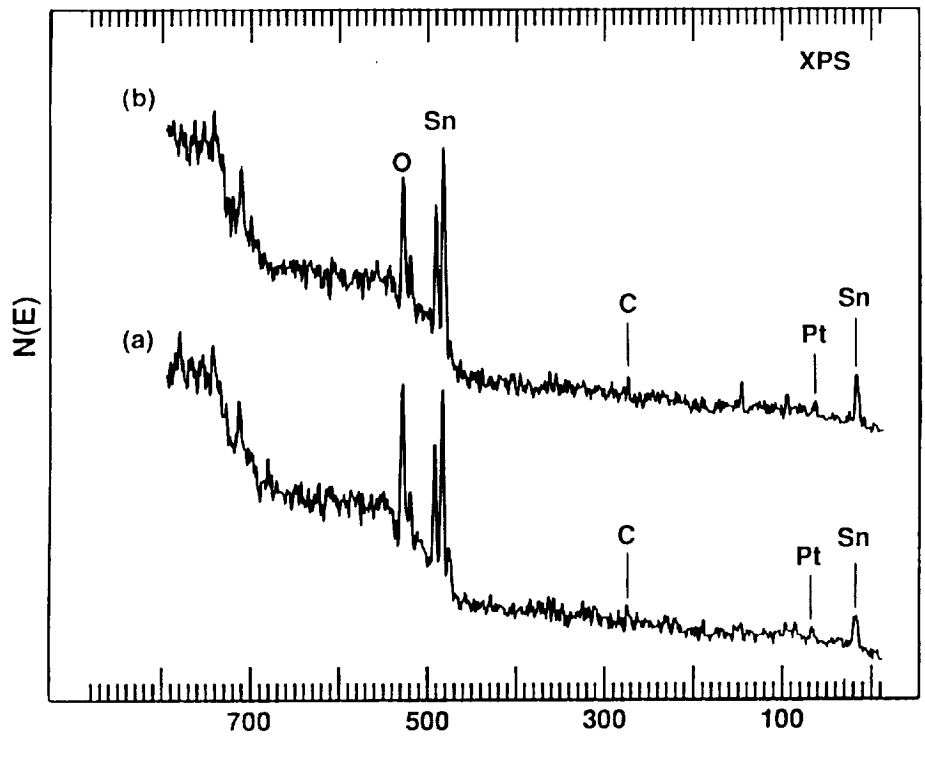

Figure 2. XPS survey spectra taken from the platinized tin oxide surface of sample B (a) before and (b) after CO reduction at 250 °C.

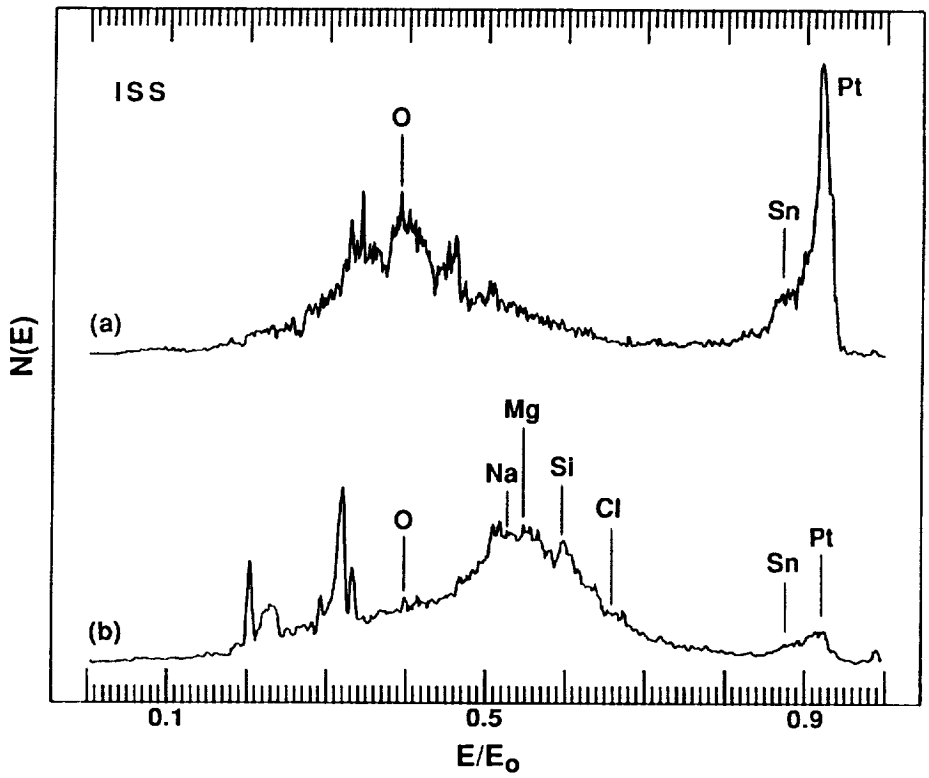

Figure 3. ISS spectra taken from sample B (a) before and (b) after CO reduction at 250 °C.

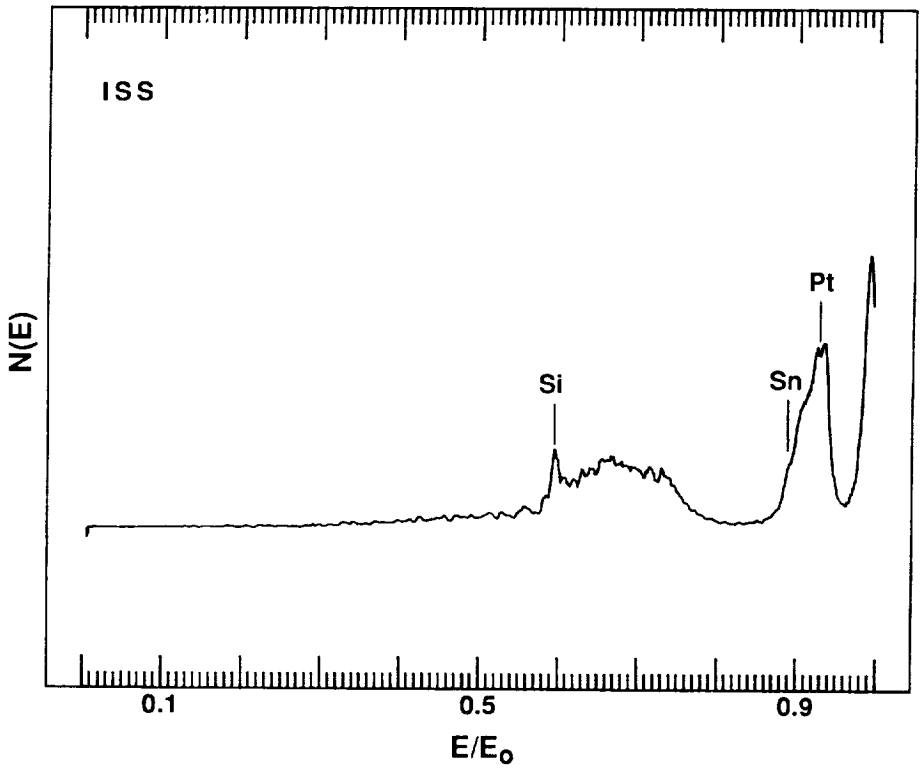

Figure 4. ISS spectrum taken from sample B after reduction and subsequent sputtering with 2 keV, 40 mA $^4He^+$ ions for 5 minutes using a beam current of 10 μA over a 1 cm^2 area.

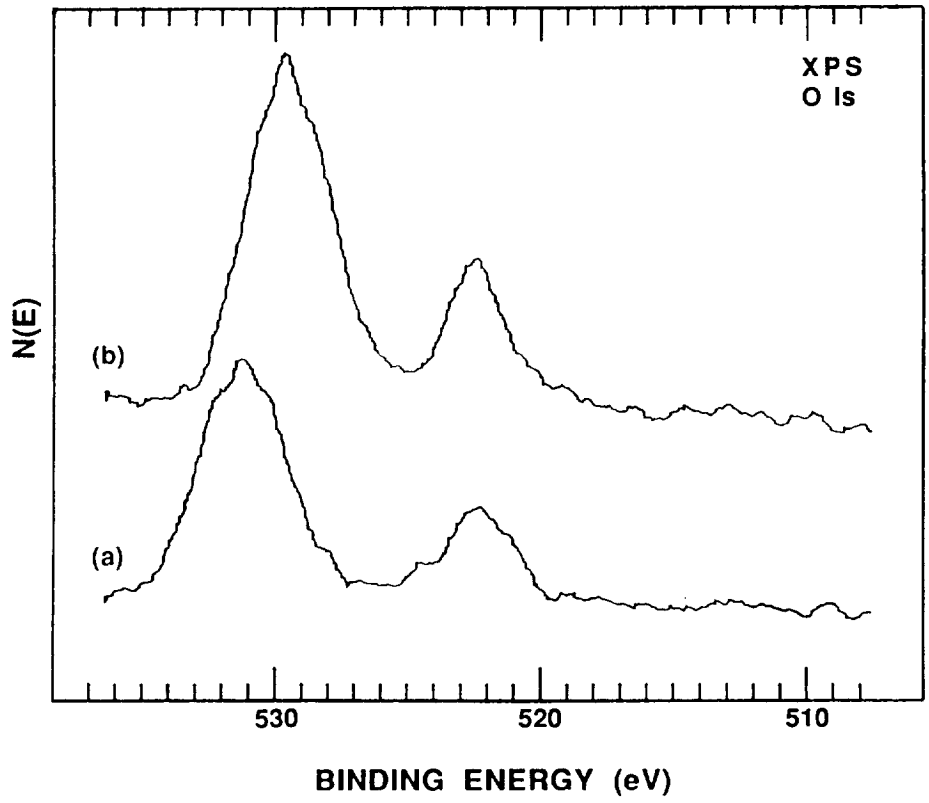

Figure 5. O 1s XPS spectra taken from sample A (a) before and (b) after CO reduction at 125 °C.

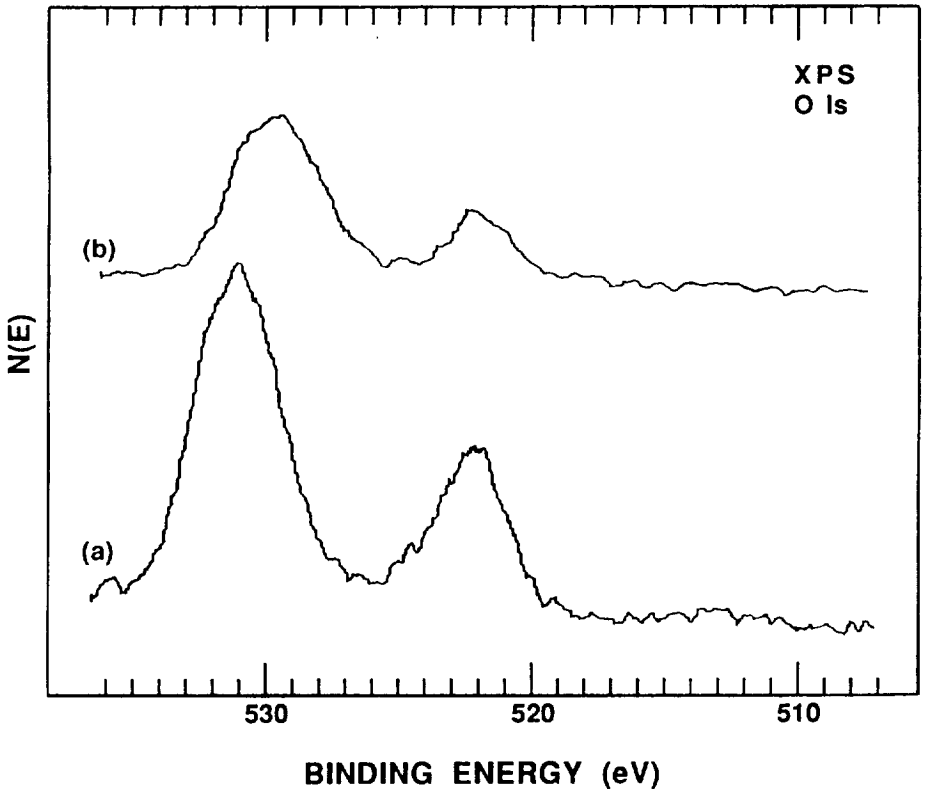

Figure 6. O 1s XPS spectra taken from sample B (a) before and (b) after CO reduction at 250 °C.

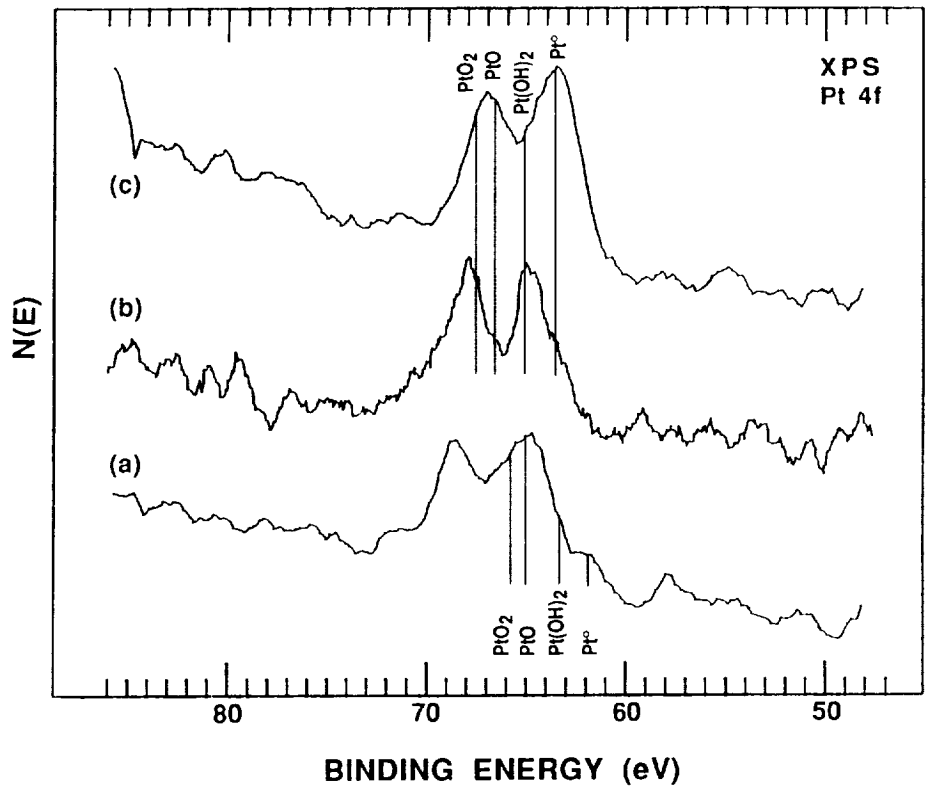

Figure 7. Pt 4f XPS spectra taken from (a) the as-entered platinized tin oxide surface, (b) sample A after CO reduction at 125 °C and (c) sample B after CO reduction at 250 °C.

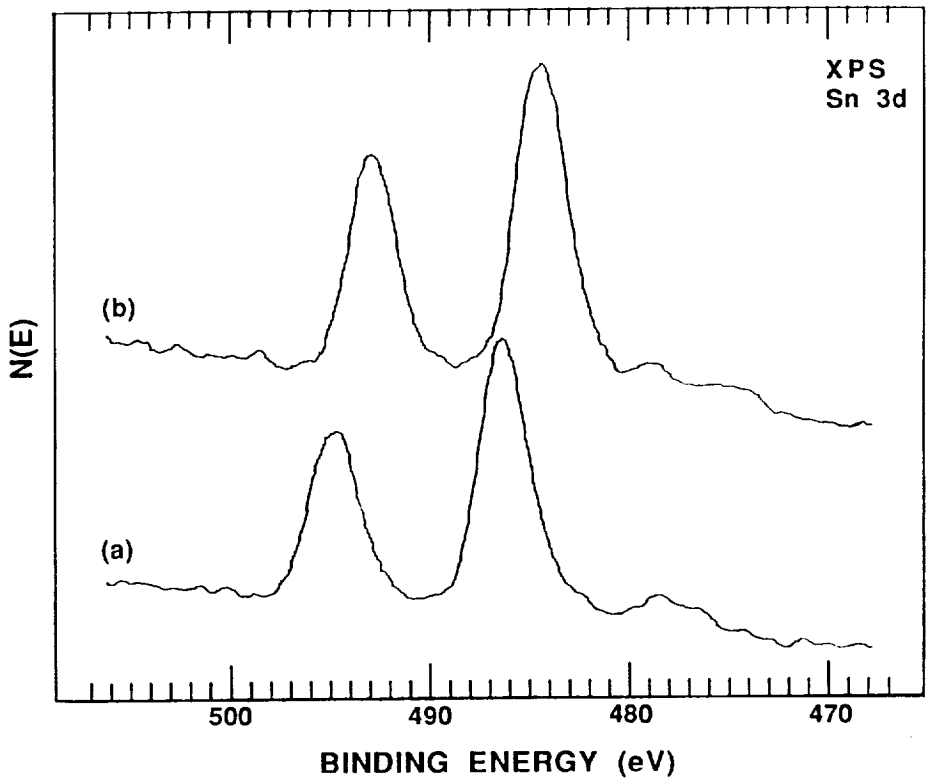

Figure 8. Sn 3d XPS spectra taken from sample A (a) before and (b) after CO reduction at 125 °C.

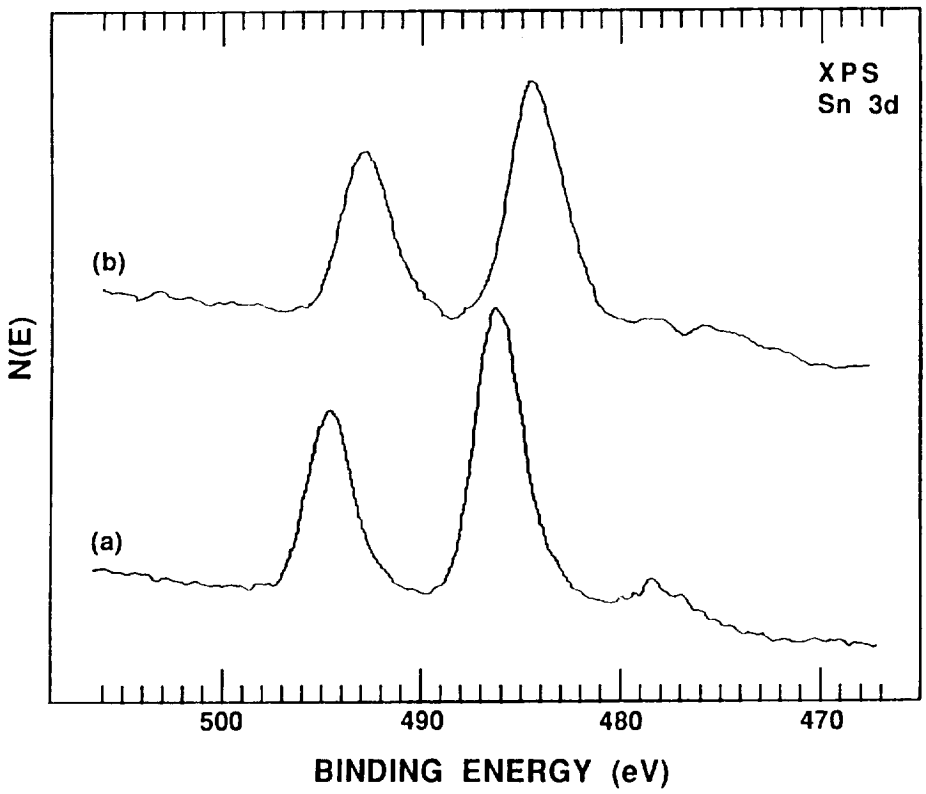

Figure 9. Sn 3d XPS spectra taken from sample B (a) before and (b) after CO reduction at 250 °C.